Chemical Physics 100 (1985) 153–169
North-Holland, Amsterdam

ENERGY BALANCE AND BRANCHING RATIOS FOR THE CHEMILUMINESCENT $Si–NO_2$ REACTION: FORMATION OF SiO $a^3\Sigma^+$, $v' \geqslant 0$, AND ULTRAFAST $a^3\Sigma^+–b^3\Pi$ E–E ENERGY TRANSFER

R. WOODWARD, J.S. HAYDEN and J.L. GOLE

High Temperature Laboratory, Center for Atomic and Molecular Science and School of Physics, Georgia Institute of Technology Atlanta, Georgia 30332, USA

Received 28 December 1984; in final form 15 May 1985

Silicon atoms react under single collision conditions with NO_2 to yield intense chemiluminescent emission from the SiO $a^3\Sigma^+–X^1\Sigma^+$ and $b^3\Pi–X^1\Sigma^+$ intercombination band systems and weak emission from the $A^1\Pi–X^1\Sigma^+$ band system. While the cross section for formation of the SiO $a^3\Sigma^+$ and $b^3\Pi$ states appears to be notably greater than that for the far more exothermic $Si+N_2O$ reaction, the observed intercombination emissions from the $Si–NO_2$ reaction involve far fewer $b^3\Pi$ vibrational quantum levels and hence considerably less spectral overlap. This facilitates the first observation of emission from SiO $a^3\Sigma^+$ vibrational quantum levels, $v' > 0$. Pressure-dependent studies demonstrate that the SiO $A^1\Pi$ and $b^3\Pi$ ($P_{\text{oxidant}} < 3 \times 10^{-4}$ Torr) states are formed in processes first order in oxidant while some collision-induced population of the very long-lived SiO $a^3\Sigma^+$ state ($v' = 0$) may occur in combination with direct product formation even at very low pressures. Temperature-dependent studies are used to indicate that reaction has occurred with ground-state Si ^3P atoms and that the SiO $b^3\Pi$ ($E_A = 4.0 \pm 1.1$ kcal/mole) and $a^3\Sigma^+$ ($E_A = 1.8 \pm 1.2$ kcal/mole) states are formed with a considerably lower activation energy than the $A^1\Pi$ state ($E_A = 7.4 \pm 1.2$ kcal/mole). The activation energy for formation of the $a^3\Sigma^+$ state, which may be negligible, is significantly smaller than that for formation of the $b^3\Pi$ state, providing some evidence for a dynamical process involving formation of $a^3\Sigma^+$ at large internuclear distance and possible subsequent transfer to $b^3\Pi$ rovibronic levels to which the $a^3\Sigma^+$ state is strongly coupled. Higher-pressure studies also provide support for this mechanism. An analysis of the weak emission from the SiO $A^1\Pi$ state allows a determination of a lower bound ($D_0^0(\text{SiO}) \geqslant 186.7 \pm 1.7$ kcal/mole) for the SiO bond energy. The controlled extension of the outlined single collision studies to elevated pressures (1) leads to a quenched SiO $A^1\Pi$ emission feature, (2) provides additional information on SiO $a^3\Sigma^+$ vibrational quantum levels, $v' > 0$ and (3) indicates, through a comparison of single and multiple collision chemiluminescent spectra, the presence of a significant ultrafast E–E transfer between the SiO $a^3\Sigma^+$ and $b^3\Pi$ states, the dominant intramolecular process corresponding to SiO $a^3\Sigma^+$, $v' = 3 + Ar \rightarrow$ SiO $b^3\Pi$, $v = 2 + Ar$.

1. Introduction

Because of the conception, based on reactant–product correlations, that the $Si–N_2O$ reaction, through spin conservation, might provide a means for selectively producing excited electronic triplet states, efforts [1–3] have focused on the characterization of this metathesis. The results have not only provided a wealth of information but also raised several questions concerning the nature of (1) the SiO triplet states formed in reaction and the coupling between these states and (2) the dynamics of the $Si–N_2O$ reaction. Silicon reacts with N_2O in a very exothermic process liberating 6.74 eV of energy of which only a maximum of 80% can be accounted in product SiO internal excitation. As we have exemplified in the previous discussion, [3] under single collision conditions, the significant energy release can result in a rather complicated and somewhat overlapped SiO spectrum. Fortunately the magnitude of the SiO bond energy provides the opportunity to study an alternate, far less exothermic, metathesis whose chemiluminescent signature is far less complicated and whose rate coefficient should exceed that for Si + N_2O [*].

We have approached the study of the Si–NO_2 reaction with the view of both simplifying and enhancing that information garnered from the study of the Si + N_2O metathesis [3]. The Si + NO_2 reaction is expected to proceed with a higher cross section and produce SiO molecules with lower internal (rovibrational) excitation. In addition, there is reason to believe that the Si–NO_2 metathesis should also proceed readily via the triplet forming process

$$\mathrm{Si}(^3\mathrm{P}) + \mathrm{NO}_2(^2\mathrm{A}_1) \rightarrow \mathrm{SiO}(\mathrm{a}^3\Sigma^+, \mathrm{b}^3\Pi, \ldots) + \mathrm{NO}(^2\Pi), \qquad (1)$$

although the formation of ground state $X^1\Sigma^+$ SiO is not precluded by spin conservation. Questions arise regarding the relative branching ratios for formation in the $a^3\Sigma^+$ and $b^3\Pi$ states (versus Si + N_2O). Under single collision conditions, the Si–NO_2 metathesis which is ≈ 5.24 eV exothermic yields emission corresponding to the SiO $a^3\Sigma^+$–$X^1\Sigma^+$ and $b^3\Pi$–$X^1\Sigma^+$ intercombination bands and very weak emission corresponding to the $A^1\Pi$–$X^1\Sigma^+$ band system. The combination of single and multiple collision studies demonstrates that the $A^1\Pi$ state is populated as a result of the reaction of silicon atoms in the high-energy tail of the silicon beam thermal distribution. The extension of the present single collision studies to multiple collision conditions thermalizing the silicon atoms to ≈ 600 K results in the complete quenching of the $A^1\Pi$–$X^1\Sigma^+$ fluorescence [6]. An analysis of the weak emission from the $A^1\Pi$ state leads to the evaluation of a lower bound for the SiO bond energy (186.7 ± 1.7 kcal/mole) in good agreement with mass spectroscopy [7].

Measured activation energies for formation of the $a^3\Sigma^+$, $b^3\Pi$ and $A^1\Pi$ states reflect the probable validity of the spin conservation implied in reaction (1) and provide some evidence for the formation of the $a^3\Sigma^+$ state at large internuclear distance and subsequent transfer to $b^3\Pi$. Because of its higher cross section and significantly smaller reaction exoergicity, the Si–NO_2 reaction provides the first opportunity to observe $a^3\Sigma^+$ vibrational quantum levels, $v \geqslant 1$. Through controlled extension to multiple collision conditions we are able to further expand our knowledge of the $a^3\Sigma^+$ state and find evidence for ultrafast energy transfer among the $a^3\Sigma^+$ and $b^3\Pi$ states.

2. Experimental

Silicon atoms distributed thermally among the ground-state $^3P_{0,1,2}$ components were reacted with NO_2 to produce an intense blue emission in a process exothermic by ≈ 5.25 eV. The metal beam was formed under single collision conditions in a beam–gas arrangement using two configurations, the first of which was identical to that described previously for our study of the Si–N_2O metathesis [3]. A second set of single collision experiments involved an oven configuration similar to that used previously for multiple collision studies [8]; the Si–NO_2 reaction was studied over the pressure range 10^{-5}–10^{-3} Torr. Silicon was vaporized over the range 1600–2050°C from a c.s. grade graphite crucible. The capped crucible was machined to fit inside a commercial tungsten basket heater (R.D. Mathis, Long Beach, CA) which was wrapped with several layers of zirconia, ZrO_2, cloth (Zircar Products, Florida, NY). The silicon vapor was reacted directly with NO_2.

We have studied the temperature dependence of the chemiluminescence from the Si–NO_2 reaction under single collision conditions [9,10]. In order to carry out these careful temperature-dependent studies, we have employed a two-step procedure [9,10]. Calibrated tungsten–rhenium thermocouples (Omega Engineering, Stamford, CT) protected by a vapor deposited tungsten sheath (Ultramet, Pacoima, CA) were first used to calibrate a Leeds and Northrup optical pyrometer. All temperatures were then measured both with the pyrometer and with the calibrated thermocouple (simultaneously), the agreement of thermocouple and pyrometer

---

[*] The Si + NO_2 reaction is far less exothermic since the O–NO bond energy exceeds that of O–N_2 by ≈ 1.5 eV. Because the NO_2 vertical electron affinity (2.36 ± 0.10 eV, ref. [4]) considerably exceeds that for N_2O (-0.15 ± 0.1 eV, ref. [5]) coulombic forces are expected to play a much larger role in this reaction.

measurements being required. Temperatures were measured to ±5°C.

Multiple collision studies were carried out with precisely that device used previously for our study of the Si–N_2O reaction. Here the metal beam was entrained in argon and this mixture subsequently oxidized. These experiments represent a direct extension of the second single collision beam–gas configuration described above in a controlled manner to multiple collision conditions. Typical operating pressures were on the order of 10–50 mTorr of oxidant and 1–1.2 Torr argon.

Again, spectra were taken with a 1 m Czerny–Turner scanning spectrometer operated in first order with a Bausch and Lomb 1200 groove/mm grating blazed at 5000 Å. An RCA 4840 photomultiplier tube was used in these experiments. The photomultiplier signal was detected with a Keithley 417 fast picoammeter whose output signal (partially damped) drove a Leeds and Northrup stripchart recorder. All spectra were wavelength calibrated.

3. Chemiluminescent spectra

The Si–NO_2 reaction is characterized by an intense blue chemiluminescence corresponding to the process

$$\mathrm{Si}(^3P_{0,1,2}) + \mathrm{NO_2}(^2A_1) \rightarrow \mathrm{SiO}(a^3\Sigma^+, b^3\Pi, A^1\Pi) + \mathrm{NO}(^2\Pi). \qquad (2)$$

The emission spectra which, under single collision conditions, extend from ≈ 2400 to 4200 Å (figs. 1, 4–6) consist of contributions from the $A^1\Pi$–$X^1\Sigma^+$, "$b^3\Pi$"–$X^1\Sigma^+$ and "$a^3\Sigma^+$"–$X^1\Sigma^+$ band systems of SiO and are dominated by the "$b^3\Pi$"–$X^1\Sigma^+$ band system onsetting at 2800 Å. The "$a^3\Sigma^+$"–$X^1\Sigma^+$ and "$b^3\Pi$"–$X^1\Sigma^+$ transitions which are nominally spin-forbidden borrow intensity through spin–orbit mixing with low-lying $A^1\Pi$ and $E^1\Sigma_0^+$ states [3]. The "$a^3\Sigma^+$" and "$b^3\Pi$" states also couple to each other and hence form a partially mixed triplet manifold with neither state of pure Σ or Π character [3]. Hence they are placed in quotes.

A significant change is observed when the low-

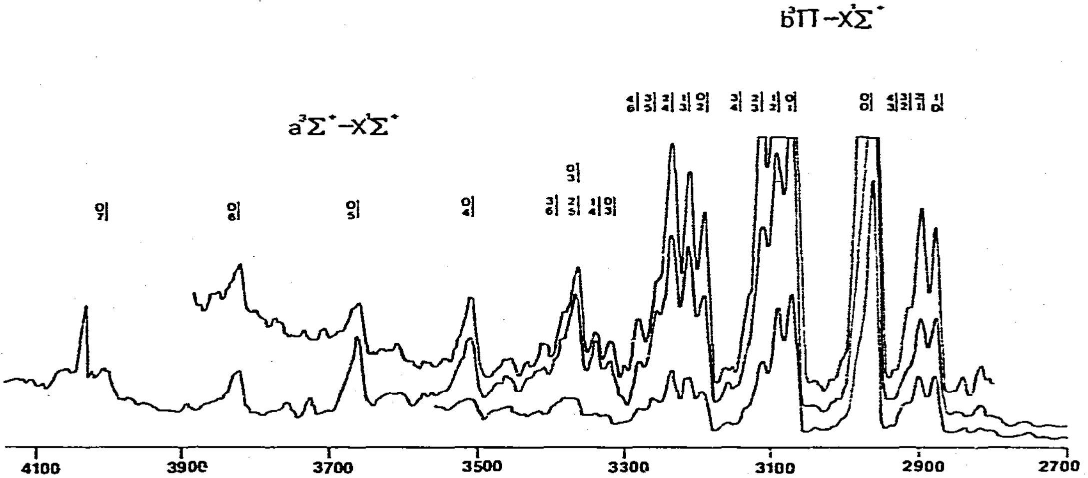

Fig. 1. Chemiluminescent spectra in the region 2700–4100 Å resulting from the reaction Si + NO_2 → SiO^* + NO recorded under "single collision" conditions as a function of increasing silicon beam temperature and metal flux. The spectrum depicts both the "$b^3\Pi$"–$X^1\Sigma^+$ and "$a^3\Sigma^+$"–$X^1\Sigma^+$ band systems. Many fewer levels of the "$b^3\Pi$" state are populated versus the observed spectrum for the Si + N_2O reaction [3]. Bandheads are designated (v', v''). The underlying continuum towards the red end of these spectra is due to blackbody radiation from the silicon cell. Spectral resolution is 10 Å. See text for discussion.

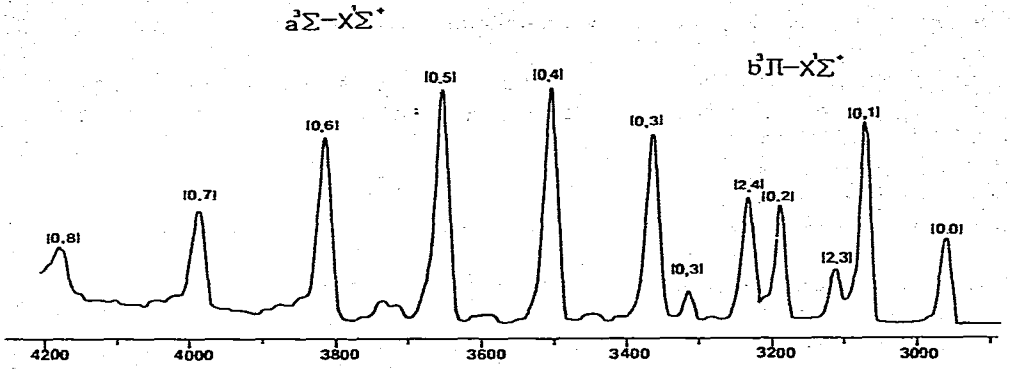

Fig. 2. Chemiluminescent spectrum in the region 2900–4200 Å resulting from reaction $Si + NO_2 \rightarrow SiO^* + NO + Ar$ recorded under multiple collision conditions. The spectrum depicts both the "$b^3\Pi$"–$X^1\Sigma^+$ and "$a^3\Sigma^+$"–$X^1\Sigma^+$ band systems. Many fewer levels of the "$b^3\Pi$" state are populated versus the single collision spectrum and emission from the "$a^3\Sigma^+$"–$X^1\Sigma^+$ band system now dominates the spectral features. The features associated with the (2, 4) and (2, 3) b–X bands have some contribution from the (0, 2) and (0, 1) a–X features respectively. Bandheads are designated (v', v''). Spectral resolution is 10 Å. See text for discussion.

pressure studies are extended to multiple collision conditions (figs. 2–4). The $A^1\Pi-X^1\Sigma^+$ band system is completely quenched and the multiple collision spectrum is dominated by the "$a^3\Sigma^+$"–$X^1\Sigma^+$ band system (fig. 2).

3.1. "$a^3\Sigma^+$"–$X^1\Sigma^+$

Readily resolvable features for the "$a^3\Sigma^+$"–$X^1\Sigma^+$ band system extend from 3300 to 4200 Å. Both the low-pressure (figs. 1 and 5) and multiple collision (figs. 2 and 3) spectra are strongly dominated by a single progression arising from the $v' = 0$ level of the $a^3\Sigma^+$ state. As figs. 3 and 5 demonstrate, the Si–NO₂ reaction which is possessed of a larger cross section and smaller reaction exoergicity than the corresponding N_2O metathesis, provides the first experimental information on vibrational levels $v' > 0$ of the $a^3\Sigma^+$ state (considerably more intense and less overlapped spectra). Therefore, using the Si + NO₂ metathesis, it has been possible to confirm and

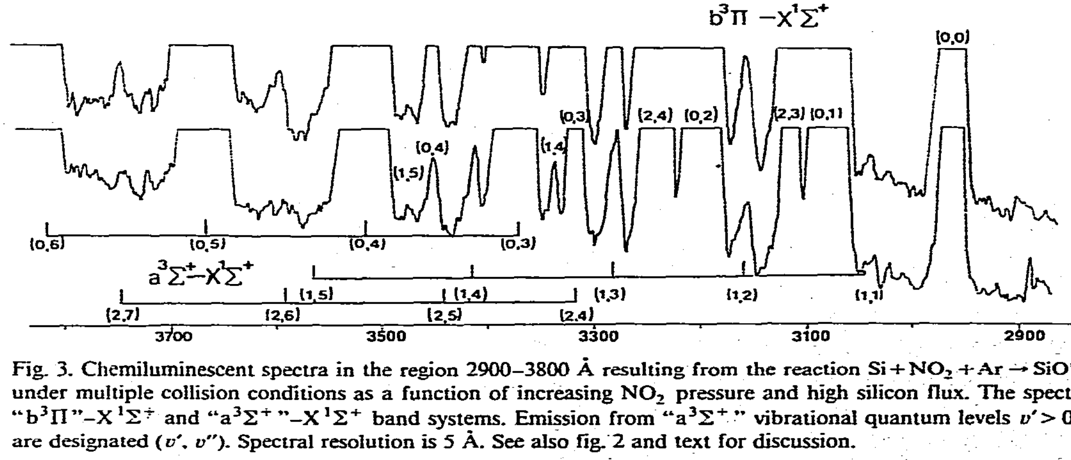

Fig. 3. Chemiluminescent spectra in the region 2900–3800 Å resulting from the reaction $Si + NO_2 + Ar \rightarrow SiO^* + NO + Ar$ recorded under multiple collision conditions as a function of increasing NO₂ pressure and high silicon flux. The spectrum depicts both the "$b^3\Pi$"–$X^1\Sigma^+$ and "$a^3\Sigma^+$"–$X^1\Sigma^+$ band systems. Emission from "$a^3\Sigma^+$" vibrational quantum levels $v' > 0$ is noted. Bandheads are designated (v', v''). Spectral resolution is 5 Å. See also fig. 2 and text for discussion.

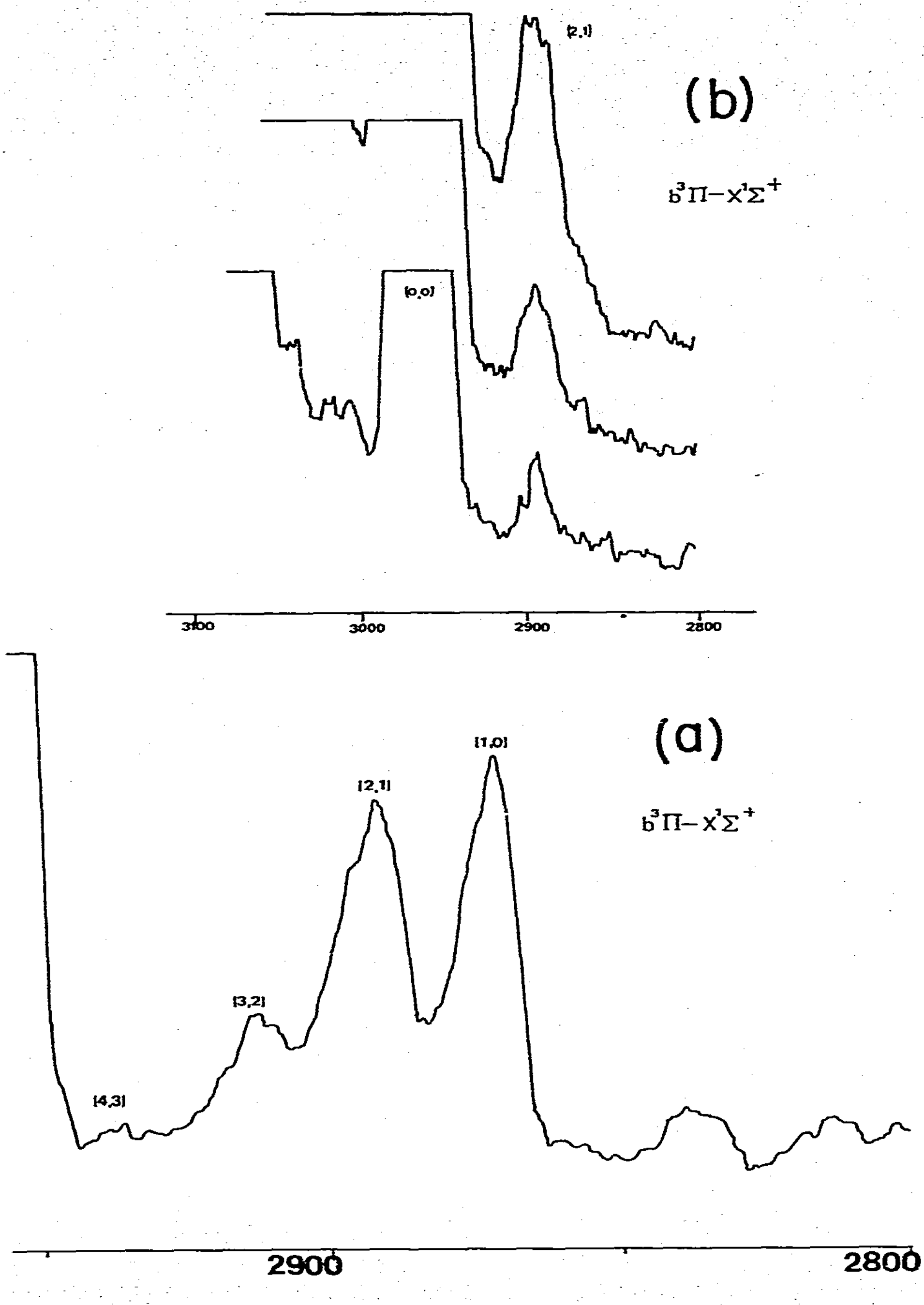

Fig. 4. Comparison of chemiluminescent spectra recorded under "single" and "multiple" collision conditions which correspond primarily to the (1, 0) sequence of the SiO "$b^3\Pi$"–$X^1\Sigma^+$ emission system; (a) single collision spectrum in the range 2800–2950 Å resulting from the reaction $Si + NO_2 \rightarrow SiO^* + NO$, (b) multiple collision spectrum in the range 2800–3100 Å corresponding to the process $Si + NO_2 + Ar \rightarrow SiO^* + NO + Ar$. Bandheads are designated (v', v''). Spectral resolution is 8 Å. Note the absence of the (1, 0), (3, 2) and (4, 3) bands in the multiple collision spectrum. See text for discussion.

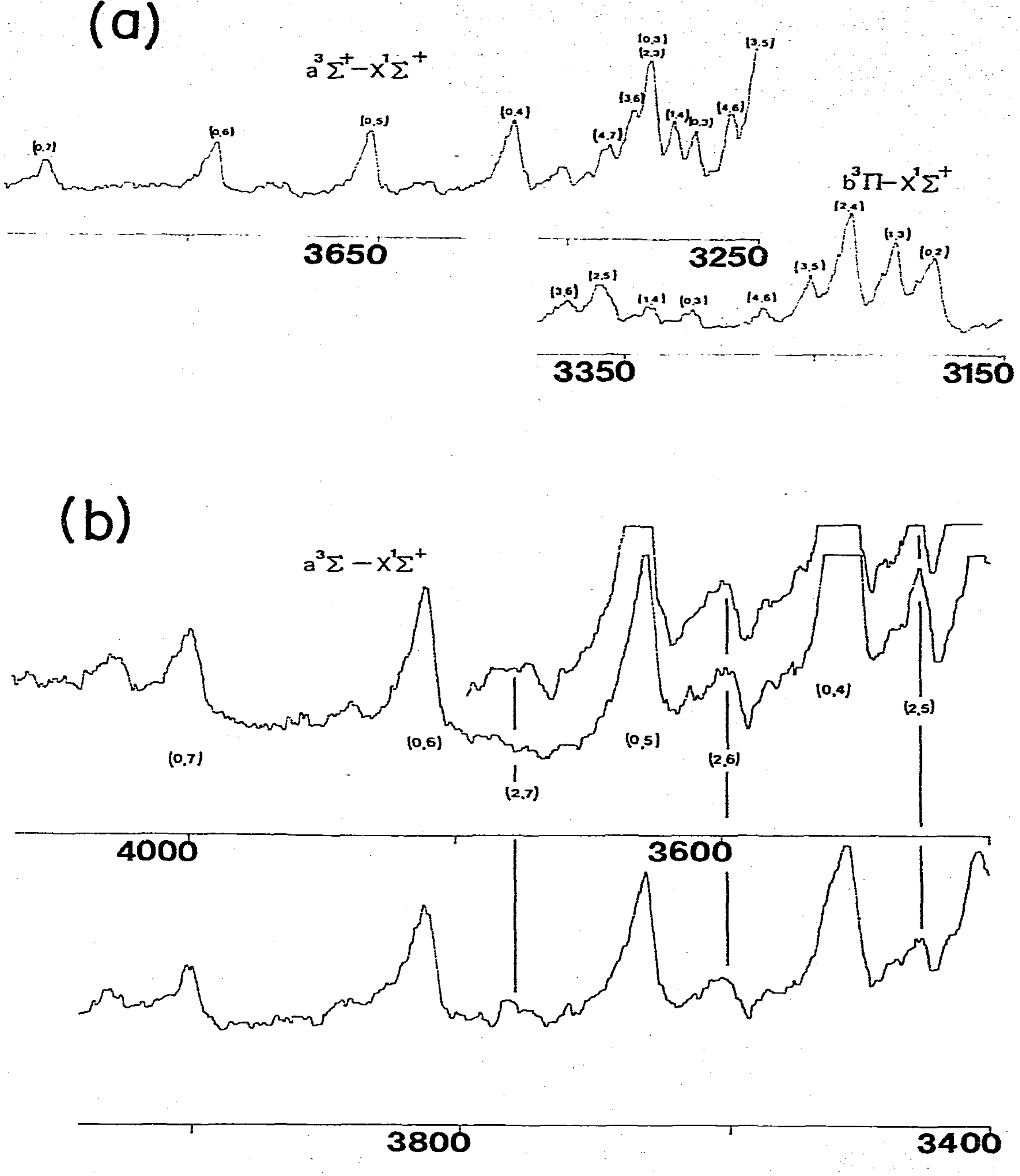

Fig. 5. Chemiluminescent spectra resulting from the reaction Si + NO_2 → SiO^* + NO recorded under "single collision" conditions illustrating portions of the "$a^3\Sigma^+$"–$X^1\Sigma^+$ band system. (a) The spectrum depicts the (0, 2) and (0, 3) sequences associated with the SiO "$b^3\Pi$"–$X^1\Sigma^+$ band system and the readily resolved emission from the "$a^3\Sigma^+$–$X^1\Sigma^+$ band system including $v' = 2$ emission bands. (b) The spectra taken as a function of increasing beam temperature and metal flux depict primarily the "$a^3\Sigma^+$–$X^1\Sigma^+$ emission region and demonstrate readily resolved emission from $v' = 0$ and $v' = 2$. Bandheads are designated (v', v''). Spectral resolution is 8 Å. See text for discussion.

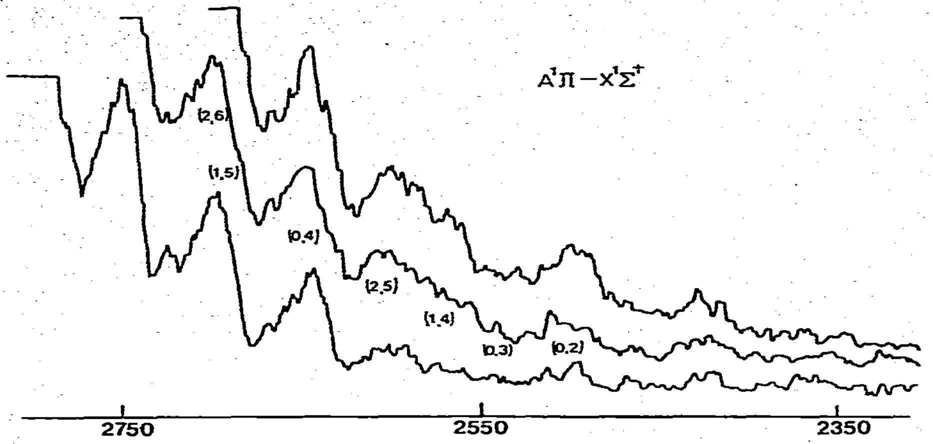

Fig. 6. Chemiluminescent spectra in the region 2300–2750 Å resulting from the reaction $Si + NO_2 \rightarrow SiO^* + NO$ recorded under single collision conditions as a function of increasing silicon beam temperature and metal flux. The observed spectrum corresponds primarily to the SiO $A^1\Pi-X^1\Sigma^+$ band system. Spectral resolution is 20 Å. See text for discussion.

somewhat refine the spectroscopic constants for the $a^3\Sigma^+$ state predicted by Field et al. [11] and complement the mapping partially determined by Linton and Capelle [2].

3.2. $b^3\Pi-X^1\Sigma^+$

Emission features corresponding to the "$b^3\Pi$"–$X^1\Sigma^+$ band system extend from ≈ 2750 to 3450 Å under single collision conditions (figs. 1, 4, 5). The spectra correspond to emission from $b^3\Pi$ quantum levels $v' = 0$–4. Under multiple collision conditions, the spectra are considerably modified, extending from ≈ 2900 to 3350 Å (figs. 2–4), and the spectrum is strongly dominated by emission from the $v' = 0$ and 2 levels although some $v' = 1$ emission is also evident. The dominance of the $v' = 0$ and 2 emission appears to result from a combination of vibrational relaxation ($v' = 0$) and ultrafast energy transfer ($v' = 2$) among the $a^3\Sigma^+$ and $b^3\Pi$ states.

3.3. $A^1\Pi-X^1\Sigma^+$

The $A^1\Pi-X^1\Sigma^+$ emission features observed only under single collision conditions in this study are depicted in fig. 6. The A–X emission characterizing the Si–NO_2 reaction is considerably weaker than that from the $a^3\Sigma^+$ and $b^3\Pi$ states and appears to result almost entirely from the reaction of silicon atoms in the high-energy tail of their thermal distribution ($T_{Si} = 2170$ K). Emission from vibrational quantum levels $v' = 0$, 1, 2 is observed.

4. Reaction kinetics

4.1. Pressure dependences

We find that the observed chemiluminescent emission from the $A^1\Pi$ and $b^3\Pi$ states of SiO increases linearly with oxidant pressure over the range 3×10^{-5}–6×10^{-4} Torr indicating that these states are formed in a process first order in NO_2. The a–X emission features ($v' = 0$ emission) while dominated by direct formation in a process first order in silicon and first order in oxidant at the lowest pressures do display some non-linear increase for pressures in excess of 1×10^{-4} Torr. The radiative lifetime of the $a^3\Sigma^+$ state is probably in excess of 10^{-2} s [☆] while the mean time

---

[☆] It is certainly longer than the radiative lifetime for the $b^3\Pi$ state which must have a larger effective transition moment. The radiative lifetime for the $b^3\Pi$ state is estimated to be 48 ms but probably is shorter [3,12]. It is likely that this represents an upper bound for the gas-phase value. Thus, a radiative lifetime in excess of 10^{-2} s for the $a^3\Sigma^+$ state is reasonable.

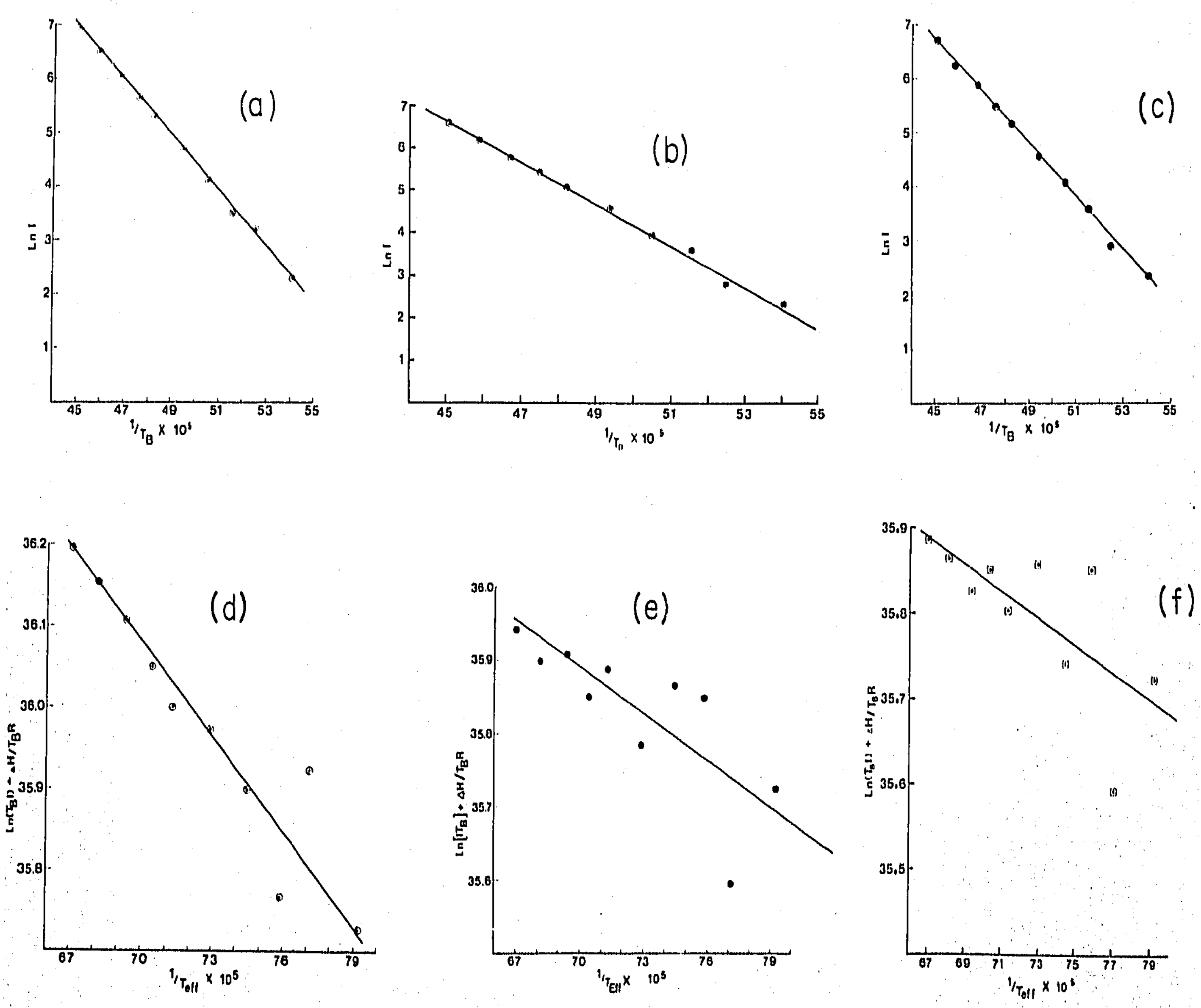

Fig. 7. Natural logarithm of relative chemiluminescent intensity versus the reciprocal of the silicon beam temperature, T_B, at (a) 2650 Å (SiO $A^1\Pi$–$X^1\Sigma^+$), (b) 3650 Å (SiO "$a^3\Sigma^+$"–$X^1\Sigma^+$), and (c) 3100 Å (SiO "$b^3\Pi$"–$X^1\Sigma^+$) and plot of $[\ln(IT_B) + \Delta H_{vap}(T_B^{mean})/RT_B]$ versus $1/T_{eff}$ for the Si + NO_2 reaction at (d) 2650 Å, (e) 3650 Å, and (f) 3100 Å corresponding to the formation of SiO* $A^1\Pi$, $a^3\Sigma^+$, and $b^3\Pi$, respectively. See text for discussion.

between collisions at 10^{-4} Torr is on the order of 10^{-3} sec. Therefore, a molecule in the $a^3\Sigma^+$ state should undergo several collisions before radiating. The monitored modification of the form of the pressure-dependent behavior will be dependent not only on the rate of vibrational deactivation but also on the dimensions of the viewing zone [3] through which one monitors the emission from the long-lived $a^3\Sigma^+$ state.

4.2. Temperature dependences – SiO ($A^1\Pi$, $a^3\Sigma^+$, $b^3\Pi$)

The results of temperature-dependence studies for the Si–NO$_2$ reaction are shown in fig. 7. The $A^1\Pi$ emission was monitored at 2650 Å corresponding predominantly to an overlap of the (0, 4) and (1, 5) bands of the $A^1\Pi$–$X^1\Sigma^+$ band system. The $a^3\Sigma^+$ emission spectrum was monitored at 3650 Å corresponding to the (0, 5) band of the "$a^3\Sigma^+$"–$X^1\Sigma^+$ band system. The $b^3\Pi$ emission system was monitored at 3100 Å corresponding to an overlap of bands in the (0, 1) sequence of the "$b^3\Pi$"–$X^1\Sigma^+$ band system. In figs. 7a–7c we plot ln I versus $1/T_B$ for the outlined selection of data. Here I is the chemiluminescent intensity and T_B is the beam (crucible) temperature. Data gathered in two runs for each band system are presented in table 1. The slope and linearity of the ln I versus $1/T_B$ plots show that the Si–NO$_2$ reaction is first order in metal flux.

Recently, a relation between the temperature dependence of the chemiluminescent intensity and the parameters of a beam–gas experiment has been formulated [9]. It is

$$-R\,\mathrm{d}(\ln I)/\mathrm{d}(1/T_B) = \Delta H_{vap} - R_{T_B} + E_A\left[\mathrm{d}(1/T_{eff})/\mathrm{d}(1/T_B)\right], \quad (3)$$

where E_A is the Arrhenius activation energy for the formation of the product whose chemiluminescence is monitored, ΔH_{vap} is the enthalpy of vaporization for the metal reacting to produce the observed chemiluminescence and

$$T_{eff} = (m_B T_G + m_G T_B)/(m_G + m_B), \quad (4)$$

where T_G is the temperature of the gas (nitrogen dioxide) and m_B and m_G are the masses of the beam atoms and gas molecules, respectively.

Eq. (3) may take into account the effect of low-lying electronic states [13] and possible reactions of dimeric and trimeric species all of which must be considered in the present study. The nature of the analysis [13] depends upon which states of the metal react to produce the observed chemiluminescence.

At 2250 K (the upper limit of the temperature-dependent studies – table 1) in excess of 99% of

Table 1
Latent heat of vaporization for silicon (^3P) and activation energy for formation of SiO* ($A^1\Pi$, $a^3\Sigma^+$, $b^3\Pi$) [a]

Reaction studied	$\Delta H_{vaporization}$ present study [b]	Temperature range (K)	Literature [c]	E_A [d]
$Si + NO_2 \rightarrow SiO^*(A^1\Pi,\ v' = 0, 1)$	105.2 ± 1.2 [e]	1850–2220	95.1	7.4 ± 1.2
$Si + NO_2 \rightarrow SiO^*(A^1\Pi,\ v' = 0, 1)$	106.8 ± 3 [e]	1880–2190	95.1	8.6 ± 3
$Si + NO_2 \rightarrow SiO^*(a^3\Sigma^+,\ v' = 0)$	97.6 ± 1.3 [f]	1850–2220	95.1	1.8 ± 1.2
$Si + NO_2 \rightarrow SiO^*(a^3\Sigma^+,\ v' = 0)$	97.1 ± 2 [f]	1880–2190	95.1	1.5 ± 2
$Si + NO_2 \rightarrow SiO^*(b^3\Pi,\ v' = 1, 2)$	100.7 ± 1.5 [g]	1850–2220	95.1	4.0 ± 1.1
$Si + NO_2 \rightarrow SiO^*(b^3\Pi,\ v' = 1, 2)$	102.0 ± 3 [g]	1880–2190	95.1	5.0 ± 3

[a] Energy in kcal/mole.

[b] Values in this column obtained from the slope of ln I versus $1/T_B$, where I is the chemiluminescent intensity and T_B is the beam temperature. The slope obtained through linear least-squares analysis is added to the value of RT_B over the temperature range of the experiment to yield a rigorous upper bound to $\Delta H_{vaporization}$ – see text for discussion.

[c] $\Delta H_{vaporization}$ at the average temperature of the experimental runs.

[d] Values in this column obtained from the slope of $[\ln(IT_B) + \Delta H_{vap}(T_B^{mean})/RT_B]$ versus $1/T_{effective}$ – see text for discussion

[e] Spectral resolution was 30 Å – data taken at 2650 Å – see text for discussion.

[f] Spectral resolution was 20 Å – data taken at 3650 Å – see text for discussion.

[g] Spectral resolution was 20 Å – data taken at 3100 Å – see text for discussion.

the reacting atoms are in the ground ^{3}P state of silicon and the single collision reaction (2) gives rise to $A^1\Pi$, $b^3\Pi$, or $a^3\Sigma^+$ chemiluminescence. The overwhelming probability for ^{3}P atom reaction as the source of the chemiluminescence can be demonstrated directly from the plots in fig. 7. In general, we expect E_A to be positive for reactions yielding chemiluminescence. Thus from eq. (3)

$$-R\,\mathrm{d}(\ln I)/\mathrm{d}(1/T_B) > \Delta H_{\mathrm{vap}} - RT_B. \qquad (5)$$

We carry out a linear least-squares analysis of the ln I versus $1/T_B$ data. The slope of the plot for the $A^1\Pi$ state in fig. 7a is -50877 ± 591 K, leading to the value 101.1 ± 1.2 kcal/mole for $-R\mathrm{d}(\ln I)/\mathrm{d}(1/T_B)$. Summing the slope energy and the value of RT_B over the temperature range of the experiment, we obtain a rigorous upper bound to ΔH_{vap}. Values obtained for two studies of emission from the $A^1\Pi$ state are given in column 2 of table 1.

The average T_B over the temperature range of the experiments was 2035 K. At these temperatures, the heat of vaporization for the equilibrium atomic vapor is 95.1 kcal/mole, only a few kcal/mole less than the observed value of $-R\,\mathrm{d}(\ln I)/\mathrm{d}(1/T_B)$ for all of the slope heats presented in column 2 of table 1. The equilibrium vapor consists of silicon atoms in the ground ^{3}P and excited ^{1}D states [14] so that ΔH_{vap} for a vapor composed solely of ground-state atoms will be slightly smaller. On the other hand, $\Delta H_{\mathrm{vaporization}}$ for forming exclusively ^{1}D atoms will be considerably higher (≈ 18 kcal/mole) [14]. The average value of RT_B over the range of the temperature-dependence studies is ≈ 4.1 kcal/mole; thus the inequality (5) holds for reaction of ground state atoms but it does not hold for reaction of excited ^{1}D atoms.

Similar arguments can be envoked when considering possible silicon dimer and trimer reaction with heats of vaporization being 112.4 [14] and 104.5 [14] kcal/mole, respectively. The inequality (5) does not hold if the metathesis producing chemiluminescence results from dimer or trimer reaction. The violation of the inequality (5) is even more pronounced if we consider the possible reaction of excited-state dimers and trimers. The observed chemiluminescence is due overwhelmingly to reaction of ground-state ^{3}P silicon atoms.

4.3. "Activation energies" for formation of SiO* $A^1\Pi$, $a^3\Sigma^+$, $b^3\Pi$

In order to evaluate the activation energies for formation of SiO* $A^1\Pi$, $a^3\Sigma^+$ and $b^3\Pi$ we rearrange the expression (3) in a manner previously described [9,10] to obtain

$$E_A \approx -\mathrm{d}\big[R\ln(IT_B) + \Delta H_{\mathrm{vap}}(T_B^{\mathrm{mean}})/T_B\big]/\mathrm{d}(1/T_{\mathrm{eff}}), \qquad (6)$$

where $\Delta H_{\mathrm{vap}}(T_B^{\mathrm{mean}})$ is the enthalpy of vaporization of the metal at the mean temperature over the range of the experiment. A selection of data for evaluating the activation energies is also plotted in fig. 7 with final results given in table 1.

It is likely that collision-induced vibrational relaxation in the $a^3\Sigma^+$ manifold (involving levels $v' > 0$) can influence the analysis of the activation energy for formation in this state. If the $v' = 0$ level is populated not only through the direct metathesis (2) but also through relaxation from higher vibrational quantum levels, the measured temperature dependence and activation energy will be affected. The long-lived $a^3\Sigma^+$ state might undergo collisions with (1) additional NO$_2$ molecules, (2) product NO molecules or (3) additional silicon beam atoms. At a constant tenuous atmosphere of reactant gas, only the NO product concentration and silicon atom concentration will increase. If these increases promote an increased vibrational relaxation through subsequent collision with the long-lived $a^3\Sigma^+$ state and the concentration of $v' = 0$ emitters increases via both direct reaction and collisional transfer, the chemiluminescent intensity will increase with increasing temperature to a greater extent than it would in the absence of vibrational relaxation. This will result in a larger slope heat and hence the prediction of a larger activation energy. Therefore, we must consider the determined activation energy for formation of the $a^3\Sigma^+$ state as a tentative upper bound to the correct activation energy. It would seem apparent that the activation energy for formation of SiO* $a^3\Sigma^+$ from the Si–NO_2 reaction is negligible.

It is clear from the data in table 1 that the $b^3\Pi$ and $a^3\Sigma^+$ states are formed with a considerably lower activation energy than the $A^1\Pi$ state. Thus there appears to be a propensity for the spin conserving process which favors formation of the $a^3\Sigma^+$ and $b^3\Pi$ states. Further, the activation energy for formation of the $a^3\Sigma^+$ state is significantly smaller than that for formation of the $b^3\Pi$ state, providing possible evidence for a dynamical process which involves formation of $a^3\Sigma^+$ at large internuclear distance and possible subsequent transfer to $b^3\Pi$ rovibronic levels to which the $a^3\Sigma^+$ state is strongly coupled (ref. [3] – table 1). As we demonstrate shortly, the extension of our single collision studies in a controlled manner to multiple collision conditions also provides support for this mechanism.

5. SiO bond dissociation energy – quenching of $A^1\Pi$ emission and energetic considerations

5.1. *Bond energy*

We have found that the Si–NO_2 reaction populates the $v' = 0, 1, 2$ levels of the SiO $A^1\Pi$ state (fig. 6) in a process whose activation energy is $\approx 7.4 \pm 1.2$ kcal/mole (table 1). Using the relationship

$$\begin{aligned} D_0^0(\mathrm{SiO}) > \underset{72.9\,[17]}{D_0^0(\mathrm{ON{-}O})} + \underset{126.7}{E_{\mathrm{int}}(\mathrm{SiO})} - \underset{0.4}{E_{\mathrm{int}}(\mathrm{Si})} \\ - \underset{0.85}{E_{\mathrm{int}}(\mathrm{NO_2})} - \underset{4.3}{E_{\mathrm{T}}^{\mathrm{i}*}} - \underset{7.4 \pm 1.2}{E_{\mathrm{A}}(\mathrm{Si{-}NO_2})} \\ = 186.65 \pm 1.7\ \mathrm{kcal/mole}^{\star}, \end{aligned} \qquad (7)$$

where $E_{\mathrm{int}}(\mathrm{Si})$, $E_{\mathrm{int}}(\mathrm{NO_2})$, and $E_{\mathrm{int}}(\mathrm{SiO})$ are the internal energies of the species in parentheses [16] $E_{\mathrm{T}}^{\mathrm{i}}$ is the relative translational energy of the reactants and $E_{\mathrm{A}}(\mathrm{Si{-}NO_2})$ is the measured activation energy of the metathesis considered [16,17] we determine a lower bound to the SiO bond energy in excellent agreement with the mass spectrometric determination of Hildenbrand [7] ($D_0^0 = 188.2$ kcal/mole). This represents the first SiO bond energy determination independent of mass spectroscopy.

5.2. *Quenching of $A^1\Pi$ fluorescence under multiple collision conditions*

The Si–NO_2 reaction is by no means sufficiently exothermic $[D_0^0(\mathrm{SiO}) - D_0^0(\mathrm{ON{-}O})]$ to populate levels of the SiO $A^1\Pi$ state. The necessary energy increment comes primarily from the combination of the reactant translational energy increment, $E_{\mathrm{T}}^{\mathrm{i}}$, and the fact that we must surmount a rather significant activation barrier in order that silicon and NO_2 react to form the $^1\Pi$ state. When taking into account the determined activation energy, we provide a correction for the possible reaction of metal atoms in the high-energy tail of their translational energy distribution. In this particular system, the SiO* molecules formed must emanate from the reaction of silicon atoms in this high-energy tail and the reactive channel is closed to silicon atoms which do not possess sufficient energy. Once the barrier is surmounted and product formation ensues, the required energy is returned and can be used for SiO $A^1\Pi$ product internal excitation.

The importance of the considered energy increments is vividly displayed if we extend our single collision studies (fig. 6) to the multiple collision pressure regime. Here the silicon beam is thermalized by a room-temperature carrier gas to temperatures ranging between 300 and 600 K. This thermalization considerably lowers $E_{\mathrm{T}}^{\mathrm{i}}$ and substantially decreases the concentration of sufficiently energetic silicon atoms. Under multiple collision conditions, no $A^1\Pi$–$X^1\Sigma^+$ emission is observed.

6. Emission features for SiO $a^3\Sigma^+$, $v > 0$

As an impetus for the present studies we had hoped to obtain information on vibrational quantum levels of the SiO $a^3\Sigma^+$ state, the emission from which was obscured in the Si–N_2O system due to overlap with notably more intense

---

☆ We determine $E_{\mathrm{int}}(\mathrm{Si})$ from a statistical average of the $^3P_0$ (0 $\mathrm{cm^{-1}}$), $^3P_1$(77.15 $\mathrm{cm^{-1}}$) and $^3P_2$ (223.31 $\mathrm{cm^{-1}}$) components of the ground ^3P state. See also ref. [16].

"$b^3\Pi$"–$X^1\Sigma^+$ emission features [3]. Therefore we chose to study a reaction which (1) should have a larger reaction cross section, (2) produce the excited triplet states of SiO and (3) produce significantly less internal rovibrational excitation in the $b^3\Pi$ state. Furhter, there is reason to believe that the Si + NO$_2$ metathesis [eq. (2)] might favor $a^3\Sigma^+$ over $b^3\Pi$ formation. As fig. 5 demonstrates, new $a^3\Sigma^+$ $v' > 0$ features can be observed under single collision conditions; however, upon extension to the multiple collision pressure regime (fig. 3) we find that (1) the $a^3\Sigma^+$ emission features are not strongly quenched but dominate those associated with $b^3\Pi$ (figs. 2 and 3) and (2) vibrational and rotational relaxation within the $b^3\Pi$ manifold further enhances spectral simplification. From the combination of the spectra in figs. 3 and 5, we record the $a^3\Sigma^+$ emission features in table 2 and determine $\omega_e = 807$ cm^{-1}, $\omega_e x_e = 5$ cm^{-1} for the $a^3\Sigma^+$ state which represents a refinement from the estimates of Field et al. [11]. The data obtained from this analysis provide a backdrop for the consideration of the ultrafast E–E energy transfer effects which manifest themselves in the observed changes in the SiO chemiluminescent spectrum as a function of increased background pressure. In table 3, we make use of our measurements of the SiO $a^3\Sigma^+$ level structure to compare the energies for several levels of the $a^3\Sigma_1^+$ and $b^3\Pi_1$ manifolds.

Table 2
Observed $v' > 0$ bandheads for SiO $a^3\Sigma^+$–$X^1\Sigma^+$

Assignment of observed bands	Wavelength (Å) [a]
(1, 1) [b]	3032
(1, 2)	3149
(1, 3)	3272
(1, 4)	3406
[(1, 5)]	3550
(2, 4) [b]	3316
(2, 5)	3450
(2, 6)	3597

[a] Approximate wavelength of bandhead – bands well fit by expression $\nu(\text{cm}^{-1}) = 33400 + 807(v') - 5(v'^2 + v') - 1241(v'') + 6(v''^2 + v'')$.

[b] (1, 0) band too weak to be observed. (2, 2) and (2, 3) bands directly under strong $b^3\Pi$–$X^1\Sigma^+$ fluorescence features. (2,1) band at frontal edge of (0, 0) band $b^3\Pi$–$X^1\Sigma^+$.

Table 3
Approximate relative energy level locations for SiO $a^3\Sigma_1^+$ and SiO $b^3\Pi_1$ manifolds, closest level separations

Levels	Energy [a] (cm^{-1})	Δ (cm^{-1})
$v = 0$, $a^3\Sigma_1^+$	33400 [b]	−433
$v = 0$, $b^3\Pi_1$	33833 [b]	
$v = 1$, $a^3\Sigma_1^+$	34197	364
$v = 0$, $b^3\Pi_1$	33833 [b]	
$v = 2$, $a^3\Sigma_1^+$	34984	154
$v = 1$, $b^3\Pi_1$	34830	
$v = 3$, $a^3\Sigma_1^+$	35761	−52
$v = 2$, $b^3\Pi_1$	35813	
$v = 4$, $a^3\Sigma_1^+$	36558	−252
$v = 3$, $b^3\Pi_1$	36810	

[a] For $a^3\Sigma_1^+$ $\nu = \nu_0 + 807(v') - 5(v'^2 + v')$.
For $b^3\Pi_1$ $\nu = \nu_0 + 1012(v') - 7.4(v'^2 + v')$.

[b] Taken from refs. [3,11].

7. Significant modifications in observed SiO triplet state spectral features as a function of pressure – the results of ultrafast intramolecular energy transfer among the excited states of SiO

Recently, we have been concerned with the characterization of ultrafast energy transfer in high-temperature systems [8]. We believe that the effects of this rapid transfer are found in those systems in which the low-lying long-lived [18] chemiluminescing triplet states of silicon monoxide are formed in a spin conserving process.

We correlate the data obtained for the SiO $a^3\Sigma^+$ state with the information first presented by Hager et al. [2] and the information on excited-state coupling discussed in ref. [3]. We consider the approximate SiO potential curves outlined in fig. 8. The $a^3\Sigma^+$ state lies at slightly lower energy and at considerably larger internuclear distance than the $b^3\Pi$ state. We believe that the location and coupling of the $a^3\Sigma^+$ and $b^3\Pi$ states has an important influence on the changes which accompany the observed chemiluminescent spectra for both the Si + NO$_2$ and Si + N$_2$O reactions as a function of increasing pressure. The Si + NO$_2$ reaction is exemplary. When this metathesis is carried out under multiple collision conditions, a major contribution to the dynamics of SiO $b^3\Pi$ formation would appear to involve the process $Si(^3P) + NO_2(^2A_1) \rightarrow SiO(a\,^3\Sigma_1^+) + NO(^2\Pi)$ at longer range, followed by conversion to SiO $b^3\Pi_1$ via a collision-induced E–E transfer. We observe the results of a process which appears to correlate with this mechanism and the near proximity of the $a^3\Sigma^+$, $v' = 3$ and $b^3\Pi$, $v = 2$ levels (table 3).

The $b^3\Pi$ state is thought to be sufficiently long-lived ($\tau_{rad} \approx 0.5$ ms) [3,11,18] that significant vibrational relaxation due to collisions manifest at relatively low pressure and before the emission of a photon. When the $b^3\Pi$ emission spectrum is obtained at very low pressures corresponding approximately to single collision conditions, the effects of vibrational relaxation are not strongly manifested (figs. 1, 4 and 5); the lower spectrum in fig. 9 is taken under near "single collision" conditions and corresponds to the (0, 0), (0, 1) and (0, 2) sequences. The bands corresponding to the (0, 2) sequence are exemplary. Under single collision conditions, we observe emission corresponding to $b^3\Pi$ vibrational levels $v' = 0$–4. As the pressure is raised to $P_{total} = 1000$ mT by entraining the silicon atoms in a carefully controlled argon pressure and subsequently oxidizing this mixture, fig. 9 demonstrates that the observed multiple collision SiO spectrum (also figs. 3 and 4) differs markedly from the single collision spectrum. The (0, 2), (0, 1) and (1, 0) (fig. 4) sequences are marked by an almost complete absence of $b^3\Pi$ emission from levels other than $v = 0$ and 2. The observed phenomena can be explained by envoking a combination of vibrational energy transfer within the $b^3\Pi$ state and ultrafast E–E transfer between the $a^3\Sigma^+$ and $b^3\Pi$ states. Because the $b^3\Pi$ state is long-lived, collisional relaxation of its vibrational manifold can occur readily on the time scale for electronic transition. In the absence of other effects, a thermalized $b^3\Pi$ state would be characterized by an overwhelming population in the $v = 0$ level; however, in this case, molecules formed at longer range in the $a^3\Sigma^+$ state find a doorway to $b^3\Pi$, $v = 2$ at $v' = 3$, $a^3\Sigma^+$ (see table 3). The efficient $a^3\Sigma^+$, $v' = 3 \rightarrow b^3\Pi$, $v = 2$, E–E transfer competes effectively with vibrational relaxation resulting in the dominance of observed emission from the $v = 0$ and 2 levels of the $b^3\Pi$ state.

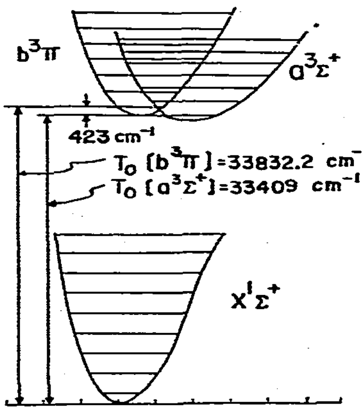

Fig. 8. Approximate potential energy curves for the $X\,^1\Sigma^+$, $a^3\Sigma^+$ and $b^3\Pi$ states of SiO, adapted from ref. [1]. See text for discussion.

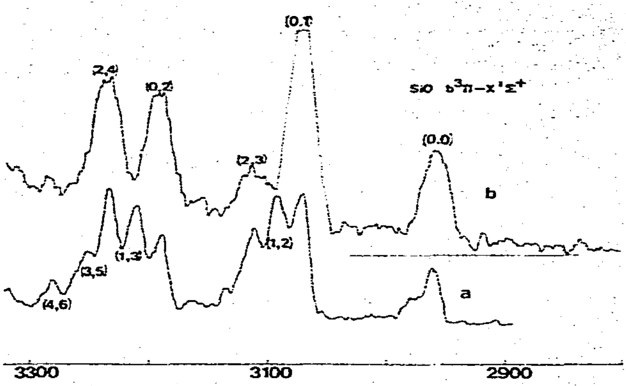

Fig. 9. Portions of chemiluminescent spectra for the reaction $Si + NO_2 \rightarrow SiO^*(b^3\Pi) + NO$ obtained under (a) "single collision" ($P_T < 10^{-3}$ Torr) and (b) multiple collision ($P_T \approx 1$ Torr) conditions. The features associated with the (2, 4) and (2, 3) b–X bands have some contribution from the (0, 2) and (0, 1) a–X features respectively. See text for discussion.

8. Discussion

8.1. Spin and angular momentum considerations

It is instructive to compare the chemiluminescent emission from the Si–NO_2 and Si–N_2O reactions especially (1) in the light of reactant–product correlations and (2) with respect to changes which accompany the observed chemiluminescence from these systems as a function of pressure. The reactions of interst are

$$\mathrm{Si}(^3\mathrm{P}_{0,1,2}) + \mathrm{N_2O}(^1\Sigma^+) \rightarrow \mathrm{SiO}(\mathrm{a}^3\Sigma^+, \mathrm{b}^3\Pi, \mathrm{A}^1\Pi) + \mathrm{N_2}(^1\Sigma_g^+) \quad (8a)$$

and

$$\mathrm{Si}(^3\mathrm{P}_{0,1,2}) + \mathrm{NO_2}(^2\mathrm{A}_1) \rightarrow \mathrm{SiO}(\mathrm{a}^3\Sigma^+, \mathrm{b}^3\Pi, \mathrm{A}^1\Pi) + \mathrm{NO}(^2\Pi). \quad (8b)$$

In the first reaction a spin "1" silicon atom interacts with a spin "0" N_2O molecule forming a spin "0" N_2 product. Given that spin conservation holds, it is predictable that the Si–N_2O reaction favors formation of triplet SiO. The silicon–NO_2 reaction is not nearly as straightforward for the spin angular momenta for silicon ($S_1 = 1$) and NO_2 ($S_2 = 1/2$) can couple to yield the resultant $S_{\text{total}} = 3/2, 1/2$. Angular momentum considerations for this reaction might favor formation of an SiO electronic state possessed of no orbital angular momentum. The experimental results appear to bear out this possibility suggesting that, at least in this reaction, there exists a propensity rule for product momenta. The Si + NO_2 reaction appears to favor, among the energetically accessible fluorescing states, formation of SiO $a^3\Sigma^+$ over SiO $b^3\Pi$ or SiO $A^1\Pi$. Such orbital angular momentum considerations do not appear to be as straightforward for the Si–N_2O reaction. The single collision spectrum [3] would seem to indicate a dominance of $b^3\Pi$ over $a^3\Sigma^+$ fluorescence, however, the relative intensity of emission from these two states might also reflect their relative radiative lifetimes. The relative intensities of the $a^3\Sigma^+$ and $b^3\Pi$ emission features for the two metatheses considered above are exemplified in fig. 10 where we focus on multiple collision spectra. Recall also that for the Si–N_2O reaction the $a^3\Sigma^+/b^3\Pi$ intensity ratio first decreases with increasing pressure reaching a minimum for $P = 5 \times 10^{-2}$ Torr and increasing for $P > 5 \times 10^{-1}$ Torr. In contrast, figs. 1, 2 and 10 demonstrate that for the Si–NO_2 reaction the $a^3\Sigma^+/b^3\Pi$ intensity ratio is somewhat larger and consistently increases as a function of increasing pressure.

Differing vibrational excitation and relaxation might also account for the observed relative $a^3\Sigma^+/b^3\Pi$ ratios. Consider that the more exothermic Si + N_2O reaction might form molecules in much higher $a^3\Sigma^+$ quantum level groupings

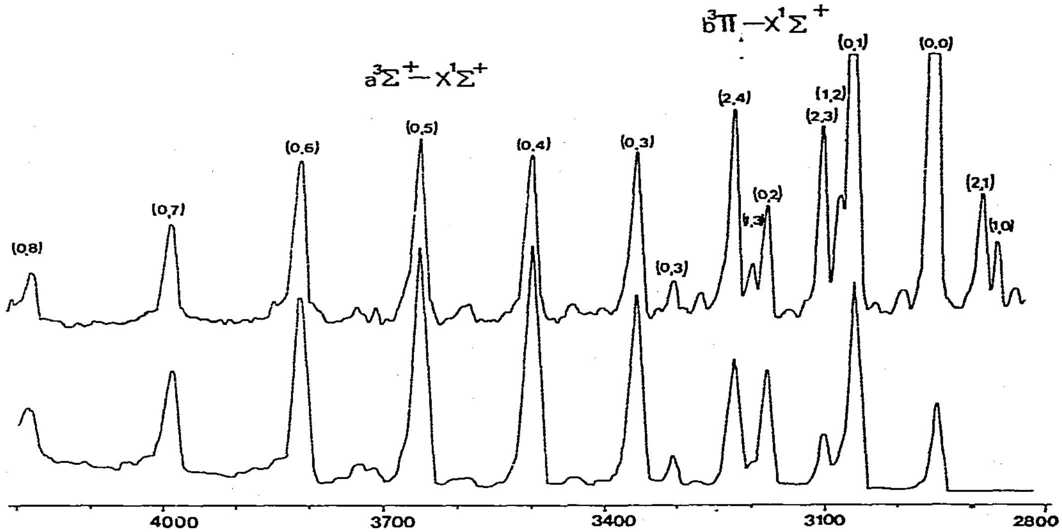

Fig. 10. Comparison of chemiluminescent spectra for the reactions (a) Si + N_2O + Ar → SiO^* + N_2 + Ar and (b) Si + NO_2 + Ar → SiO^* + NO + Ar taken under multiple collision conditions ($P_T \approx 1$ Torr). See text for discussion.

than does Si + NO_2. The emission from high $a^3\Sigma^+$ vibrational levels is likely obscured due to a significantly larger $b^3\Pi$–$X^1\Sigma^+$ transition moment. Vibrational relaxation to $v' = 0$ might be more readily accomplished in the Si–NO_2 system if the distribution of (nascent product) populated $a^3\Sigma^+$ vibrational quantum levels corresponds to a much lower quantum number grouping than that for Si + N_2O. Thus, there appear to be at least two possible reasons why the emission from the "$a^3\Sigma^+$"–$X^1\Sigma^+$ band system dominates that from the "$b^3\Pi$"–$X^1\Sigma^+$ band system for the Si + NO_2 reaction.

Because of the increased dominance of the $a^3\Sigma^+$ fluorescence features relative to those for $b^3\Pi$, the Si + NO_2 + Ar system can provide a more prolific source of $a^3\Sigma^+$, $v' = 0$ for a chemically driven-energy transfer laser system [3]. We must note that the dominance of $a^3\Sigma^+$ over $b^3\Pi$ emission demonstrated in figs. 2 and 10 is most likely muted because of a much longer $a^3\Sigma^+$ radiative lifetime (versus $b^3\Pi$). In fact, it is not clear that the dominance of the $b^3\Pi$ emission features in the spectra resulting from the Si–N_2O reaction indicates that the $b^3\Pi$ population exceeds that for $a^3\Sigma^+$. Since both the $a^3\Sigma^+$ and $b^3\Pi$ radiative lifetimes are long versus the time for traversal through the viewing zone, the $a^3\Sigma^+$ emission features are affected as the result of both the smaller transition moment for the $a^3\Sigma^+$ versus the $b^3\Pi$ state and because a significantly larger number of $a^3\Sigma^+$ molecules will diffuse out of the viewing zone before emission of : photon. On the other hand, the system (spectrometer + phototube + ...) has a more sensitive response in the $a^3\Sigma^+$ emission region, partially counteracting the effects of radiative lifetime.

The apparent spin and orbital angular momentum propensities which characterize the Si–NO_2 and Si–N_2O reactions are also found to be manifested in the Si–O_3 metathesis

$$\mathrm{Si}(^3P) + \mathrm{O_3}(^1A_1) \rightarrow \mathrm{SiO}^*(A^1\Pi,\ a^3\Sigma^+,\ b^3\Pi) + \mathrm{O_2}(^3\Sigma_g^-). \qquad (9)$$

Here, we find [19] that SiO* $A^1\Pi$ emission strongly dominates fluorescence from the $a^3\Sigma^+$ and $b^3\Pi$ states. This could be predicted on the basis of spin conservation and what are apparently similar orbital angular momentum propensities to those for the Si–NO_2 metathesis. (Here, however, we find a dominance of the $\Omega = 1$ component.) Further, we find no evidence for population of the SiO $E^1\Sigma_0^+$ state.

8.2. *Activation energy partitioning*

The measured activation energies for formation of the SiO $a^3\Sigma$, $b^3\Pi$ and $A^1\Pi$ states would appear to suggest (1) a set of propensity rules for product spin and orbital angular momentum and (2) in conjunction with the present multiple collision studies, the importance of the "large r" $a^3\Sigma^+$ state as an intermediate for the formation of SiO $b^3\Pi$ molecules.

The Si ^3P state is divided into three fine-structure components and there are possible questions concerning their relative contribution to the observed activation energy. If during the course of the chemiluminescence experiment, the change in the state distributions of the reactants as a function of temperature does not alter the reaction rate, and if there is no reaction selectivity with respect to a particular spin–orbit component, the experimentally measured activation energy can be expressed as

$$E_A\,|l\rangle = \left(\langle E_{\mathrm{trans}}\rangle^{|l\rangle^*} - \langle E_{\mathrm{trans}}\rangle^{|l\rangle}\right), \qquad (10)$$

where $\langle\ \rangle^{|l\rangle^*}$ denotes the average of all atom–molecule interactions leading to formation of product in state $|l\rangle$ and $\langle\ \rangle^{|l\rangle}$ denotes the average over all atom–molecule interactions (i.e. the thermal average). If one of the spin–orbit components reacts more readily with the NO_2 molecule, eq. (10) must be appended and the measured activation energy, $E_A\,|l\rangle$, must also take into account the internal energy of the beam atoms. However, the maximum correction to the partition of the measured activation energy for the Si–NO_2 interaction over the temperature range is -0.60 kcal/mole for exclusive reaction with $^3P_0$ Si atoms and 0.30 kcal/mole for exclusive reaction with $^3P_2$ Si. Thus, the activation energies presented in table 1 bear primarily the significance expressed in eq. (10) with, at best, a small adjustment for internal state corrections [6,17].

The apparently small if not negligible activation energy for formation in the SiO $a^3\Sigma^+$ state corresponds to an activation energy for product SiO which is less than or equal to that for the formation of product molecules in any electronic states of the system. This, of course, includes the ground $X^1\Sigma^+$ state. This result thus indicates that the formation of molecules in the $a^3\Sigma^+$ state can compete effectively with ground-state formation, a situation which signals the possibility of a population inversion.

8.3. Energy balance, population of SiO $A^1\Pi$ and $b^3\Pi$ states – possible $b^3\Pi$ vibrational relaxation at low pressure

We have used the observed weak emission from the $v' = 0$, 1, 2 levels of the SiO $A^1\Pi$ state to deduce a lower bound for the SiO bond energy. As we have done previously for the Si + N_2O reaction [3], we also consider the energy balance involving populated levels of the $b^3\Pi$ state. The highest level from which emission in the $b^3\Pi$ state is observed corresponds to $v = 4$. The available energy to populate the $b^3\Pi$ state is

$$\begin{aligned} E_{\text{available}} &= \underset{65827}{D_0^0(\text{SiO})} - \underset{25498}{D_0(\text{NO}_2)} + \underset{298}{E_{\text{int}}(\text{NO}_2)} \\ &\quad + \underset{145}{E_{\text{int}}(\text{Si})} + \underset{1505}{E_{\text{T}}^{\text{i}}} + \underset{1400}{E_{\text{A}}(\text{b}^3\Pi)} \\ &= 43672\ \text{cm}^{-1}. \end{aligned}$$

The energy increment corresponding to $v = 4$, $b^3\Pi$ is 37741 cm^{-1}. The energy differential, 5931 cm^{-1}, indicates that approximately six more levels in the SiO $b^3\Pi$ state might be populated due to reaction exothermicity. This may be a real energy discrepancy or it might result in part from vibrational relaxation in the $b^3\Pi$ manifold even at very low pressure.

8.4. Ultrafast energy transfer – possible implications for previous studies of silicon oxidation

We believe that the phenomena of ultrafast energy transfer can account for Hager et al.'s [1] observation of "an anomalously high intensity for the emission from the $b^3\Pi$ $v = 2$ bands relative to the $v = 1$ bands". It is surprising that these effects do not manifest themselves strongly in the studies of Linton and Capelle [2], however, although these authors did not observe a complete cutoff of the emission bands for the $b^3\Pi$ state at $v = 2$ (Hager et al. [1]), they do indicate a considerable decrease in intensity for those bands $v > 3$, consistent with the data obtained and conclusions drawn in the present study. Note also that fig. 10 demonstrates a significant $v = 1$ $b^3\Pi$ spectral component for the Si + N_2O reaction versus its almost complete absence for Si + NO_2.

Acknowledgement

It is a pleasure to acknowledge the National Science Foundation and the Department of Energy, METC for partial support of this research.

References

[1] G. Hager, R. Harris and S.G. Hadley, J. Chem. Phys. 63 (1975) 2810;
G. Hager, L.E. Wilson and S.G. Hadley, Chem. Phys. Letters 27 (1974) 439.

[2] C. Linton and G.A. Capelle, J. Mol. Spectry. 66 (1977) 62.

[3] J.L. Gole and G.J. Green, Chem. Phys. 100 (1985) 133.

[4] E. Herbst, T.A. Patterson and W.C. Lineberger, J. Chem. Phys. 61 (1974) 1300.

[5] J.S. Nalley, R.N. Compton, H.C. Schweinler and V.E. Anderson, J. Chem. Phys. 59 (1973) 4125.

[6] G.J. Green and J.L. Gole, Chem. Phys. 46 (1980) 67.

[7] D.L. Hildenbrand, High Temp. Sci. 4 (1972) 244.

[8] D.M. Lindsay and J.L. Gole, J. Chem. Phys. 66 (1977) 3886;
M.J. Sayers and J.L. Gole, J. Chem. Phys. 67 (1977) 5442;
J.L. Gole and S.A. Pace, J. Chem. Phys. 73 (1980) 836;
A.W. Hanner and J.L. Gole, J. Chem. Phys. 73 (1980) 5025.

[9] D.R. Preuss and J.L. Gole, J. Chem. Phys. 66 (1977) 880, 2994.

[10] J.L. Gole and D.R. Preuss, J. Chem. Phys. 66 (1977) 3000.

[11] R.W. Field, A. Lagerqvist and I. Renhorn, Physica Scripta 14 (1976) 298.

[12] B. Meyer, J.J. Smith and K. Spitzer, J. Chem. Phys. 53 (1970) 3616.

[13] L.H. Dubois and J.L. Gole, J. Chem. Phys. 66 (1977) 779.

[14] R. Hultgren, P.D. Desai, D.T. Hawkins, M. Gleiser, K.K. Kelley and D.D. Wagman, Selected values of the thermo-

dynamic properties of the elements (American Society for Metals, Metals Park, 1973);
C.E. Moore, Atomic energy levels, Vol. 1, NSRDS-NBS 35 (1971).
[15] J. Pfeifer, G. Green and J.L. Gole, High Temp. Sci. 17 (1984) 85.
[16] P.J. Dagdigian, H.W. Cruse and R.N. Zare, J. Chem. Phys. 62 (1973) 1824;
J.L. Gole and R.N. Zare, J. Chem. Phys. 57 (1972) 5331;
R.N. Zare, Ber. Bunsenges. Physik. Chem. 78 (1974) 153;
D.R. Stull and H. Prophet, eds., JANAF thermochemical tables, 2nd Ed., NSRDS-NBS 37 (1971).
[17] D.R. Preuss and J.L. Gole, J. Chem. Phys. 66 (1977) 880.
[18] W.H. Smith and H.S. Liszt, J. Quant. Spectry. Radiative Transfer 12 (1972) 505.
[19] G.J. Green, B. Cardelino and J.L. Gole, unpublished results.